Supplemental Figure Legends

Supplemental Figure 1. Cytokines and chemokines in mouse BALF before and after ischemia. Donor mice were administered low dose of lipopolysaccharide (LPS) intratracheally and then transplanted into allogeneic recipients. CXCL2, CXCL1, CXCL10 and TNFα levels were measured in BALF before and after ischemia (n =4-10). Graphs were analyzed by unpaired t-test. n.s. not significant; *p<0.05; ****p<0.0001.

Supplemental Figure 2. Analysis of human donor lung and recipient gut microbiome. Ten bronchoalveolar lavage (BAL) washings of donor lungs were obtained in the operating room at the time of organ implantation. Rectal swabs were obtained for five of these patients at the same time. Samples were immediately centrifuged to collect cellular DNA and stored at -80° C. Samples then underwent batched genomic DNA extraction, PCR-amplification targeting the 16S ribosomal RNA gene, pooling, and high-throughput sequencing with paired-end, 300 base reads on the Illumina MiSeq platform to obtain overall taxonomic compositions of the microbial communities. A sterile swab obtained just prior to DNA extraction was used for the negative control. Distances for each sample's overall microbial profile were generated via square root transformation of the relative abundances of each taxon. A non-metric multidimensional scaling plot was created by using Bray-Curtis dissimilarity through PRIMER version 7 as shown in Supplemental Figure 2. 2D stress was 0.14. An analysis of similarity (ANOSIM) was used to determine statistical similarities between groups.

Supplemental Figure 3. LPS administration induces lung injury. Wild-type C57BL/6 mice were intratracheally treated with LPS (2µg/g BW) and lung injury was assessed 24 h post LPS infection. (A) Quantification of neutrophil infiltration into lungs treated with LPS compared to untreated naïve mice (n=5). Neutrophils were gated on live $CD45^+Ly6G^+CD11b^+CD24^+/SSC^{hi}$. (B) Percentage of extravasated neutrophils into lungs treated with LPS compared to untreated naïve mice measured by IV injection of APC-conjugated anti-CD45 3 min prior to euthanasia (n=5-7). (C) Lungs were weighed before and after oven desiccation (>72 h) and the final wet-to-dry lung ratio was calculated (n=5-7). (D) Histopathological analysis of H&E stained lung tissue. Photomicrographs are representative from 3–5 mice. Bar = 100 µm. All graphs show means ± SD. Graphs were analyzed by unpaired t-test.**p<0.01;****p<0.0001.

Supplemental Figure 4. *Tlr4* expression in the alveolar compartment is restricted to alveolar macrophages. UMAP plots (A, C, E) and feature plots (B, D, F) showing specific cell populations and expression of *Tlr4* in three published scRNA-seq datasets. A, B: Reyfman et al., AJRCCM, 2019. C, D: Habermann et al., bioRxiv, 2019. C.D: Madissoon et al., Genome Biol, 2019.

Supplemental Figure 5. IT clodronate-loaded liposomes (Clo-lip) selectively deplete tissue-resident alveolar macrophages (TRAM) *in vivo* without affecting other cell types. (A) Representative flow diagram of TRAM gated as live $CD45^+Ly6G^-NK1.1^-SiglecF^+CD64^+$ along with efficient depletion of TRAMs in WT mice. (B) Quantification of TRAM expression in lungs treated with IT PBS-lip or Clo-lip (n=5-6). (C) Percentage of extravasated neutrophils into lungs treated with IT PBS-lip or Clo-lip measured by IV injection of APC-conjugated anti-CD45 3 min prior to euthanasia (n=5-11). (D) Quantification of Dendritic cells (DC), non-classical monocytes (NCM) and classical monocytes (CM) in lungs treated with IT PBS-lip or Clo-lip. Cells were gated as live $CD45^+Ly6G^-NK1.1^-SiglecF^-CD64^-CD11b^+$ monocytes of which $Ly6C^{high}MHCII^{+/-}$, $Ly6C^{low}MHCII^-$ and $Ly6C^-MHCII^-$ were identified as CM, NCM and $CD11b^+$DC, respectively (n=4-11). All graphs show means ± SD. Graphs were analyzed by unpaired t-test. n.s. not significant; ****p<0.0001.

Supplemental Figure 6. Neutrophil influx after LPS stimulation is independent of classical monocytes (CM), non-classical monocytes (NCM) and dendritic cells (DC). Representative flow diagrams gated as live $CD45^{+}Ly6G^{-}NK1.1^{-}SiglecF^{-}CD64^{-}CD11b^{+}$ monocytes of which $Ly6C^{high}MHCII^{+/-}$, $Ly6C^{low}MHCII^{-}$ and $Ly6C^{-}MHCII^{-}$ were identified as CM, NCM and $CD11b^{+}$DC, respectively. (A, B) Representative gating and quantification of CM after injection of antibody against CCR2 (n=5-6). (C) Quantification of neutrophil infiltration into lungs in CM-depleted compared to IgG control mice 24 h following LPS-IT (n=4-6). Neutrophils were gated on live $CD45^{+}Ly6G^{+}CD11b^{+}CD24^{+}/SSC^{hi}$. (D, E) Representative gating and quantification of NCM after IV PBS-lip or Clo-lip (n=2-4). (F) Quantification of neutrophil infiltration into lungs in NCM-depleted compared to PBS control mice 24 h following LPS-IT (n=2-3). Neutrophils were gated as on (C). (G) Quantification of $CD11b^{+}$DC using the CD11b-DTR system (n=3). (H) Quantification of neutrophil infiltration into lungs in $CD11b^{+}$DC -depleted compared to PBS control mice 24 h following LPS-IT (n=2-3). Neutrophils were gated as on (C). All graphs show means ± SD. Graphs were analyzed by unpaired t-test. n.s. not significant; *p,0.05; **p<0.01.

Supplemental Figure 7. Levels of endotoxin used in *in vitro* are similar to *in vivo* data. TRAM were harvested from BALF of wild type C57BL/6 mice and incubated *in vitro* with the depicted amount of LPS. The concentration of 0.01 µg/mL gave the same EU/mL in the culture media than the in vivo experiments measured by ELISA.

Supplemental Figure 8. TLR4 expression in TRAM harvested from BALF of pre-ischemia, 1h, 4h, and 24h post-ischemia. TLR4 was visualized by immunofluorescence using a specific PE-TLR4 antibody. In pre-ischemia and 1 h post-ischemia TLR4 (red) is localized in the perinuclear area. TLR4 translocated to the plasma membrane after 4 and 24 h post-ischemia. Images acquired using a Zeiss Axio Imager Z2 with ApoTome.2, Plan-Apochromat 100x/1.40 objective. Bar = 10 µm.

Supplemental Figure 9. Three-dimensional representation of Z-stacks of TLR4 expression in TRAM harvested from BALF of pre-ischemia, 1h, 4h, and 24h post-ischemia. TLR4 was visualized by immunofluorescence using a specific PE-TLR4 antibody. In pre-ischemia and 1 h post-ischemia TLR4 (red) is localized in the perinuclear area. TLR4 translocated to the plasma membrane after 4 and 24 h of post-ischemia. Three-dimensional images acquired using a Zeiss Axio Imager Z2 with ApoTome.2, Plan-Apochromat 100x/1.40 objective and visualized using Zen 2.3 software. Z-stacks= 12 slides at 2-4 µm steps.

Supplemental Figure 10. Exogenous ROS stimulate TLR4 translocation to the plasma membrane without affecting mRNA levels at 1h. (A) Expression level of *Tlr4* mRNA in TRAM harvested from WT BALF and treated in vitro with 100 µM H_2O_2 for 1h (n=3). (B) Protein expression of TLR4 at the plasma membrane in TRAM harvested and treated as in (A), assessed by flow cytometry (n=3). (C) % Viability of TRAM harvested as in (A) and treated in vitro with 100 µM H_2O_2 for 1h, 4h and 6h. All graphs show means ± SD. (A) and (B) graphs were analyzed by unpaired t-test. (C) Graph was analyzed by one-way Anova followed by Tukey's post-hoc test. n.s. not significant; *p<0.05;****p<0.0001.

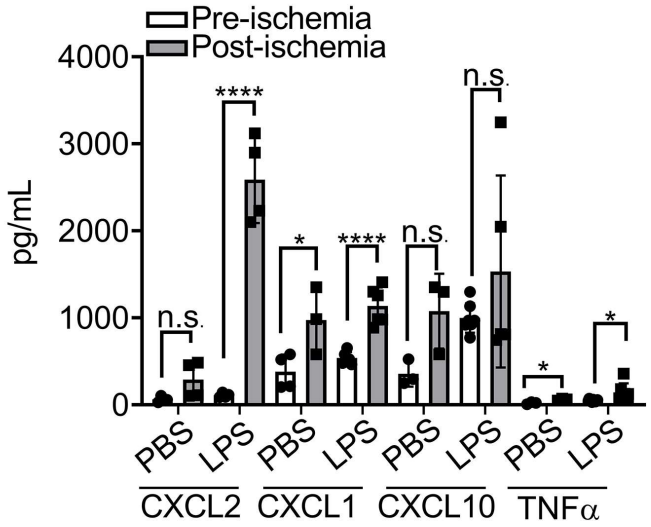

Suppl Figure 1

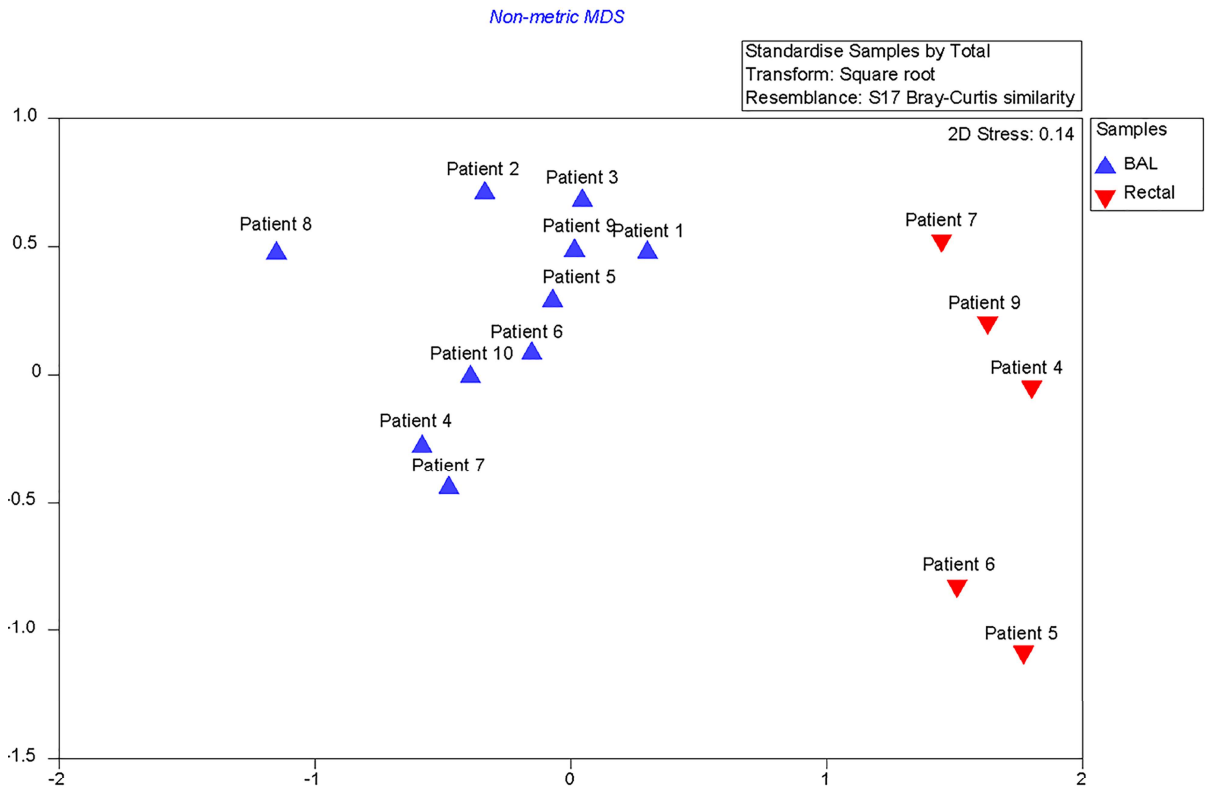

Suppl Figure 2

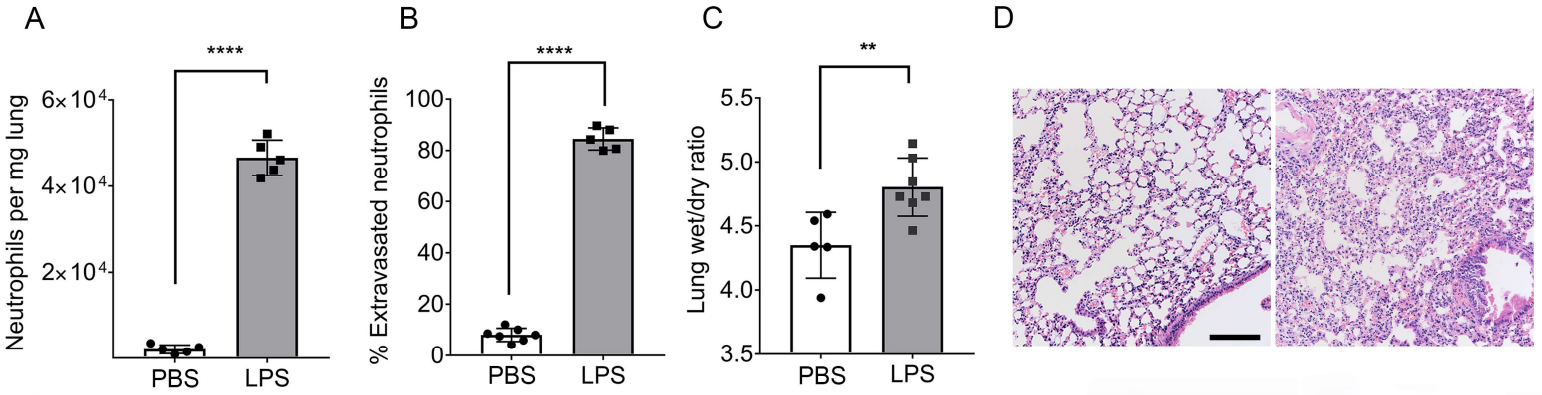

Suppl Figure 3

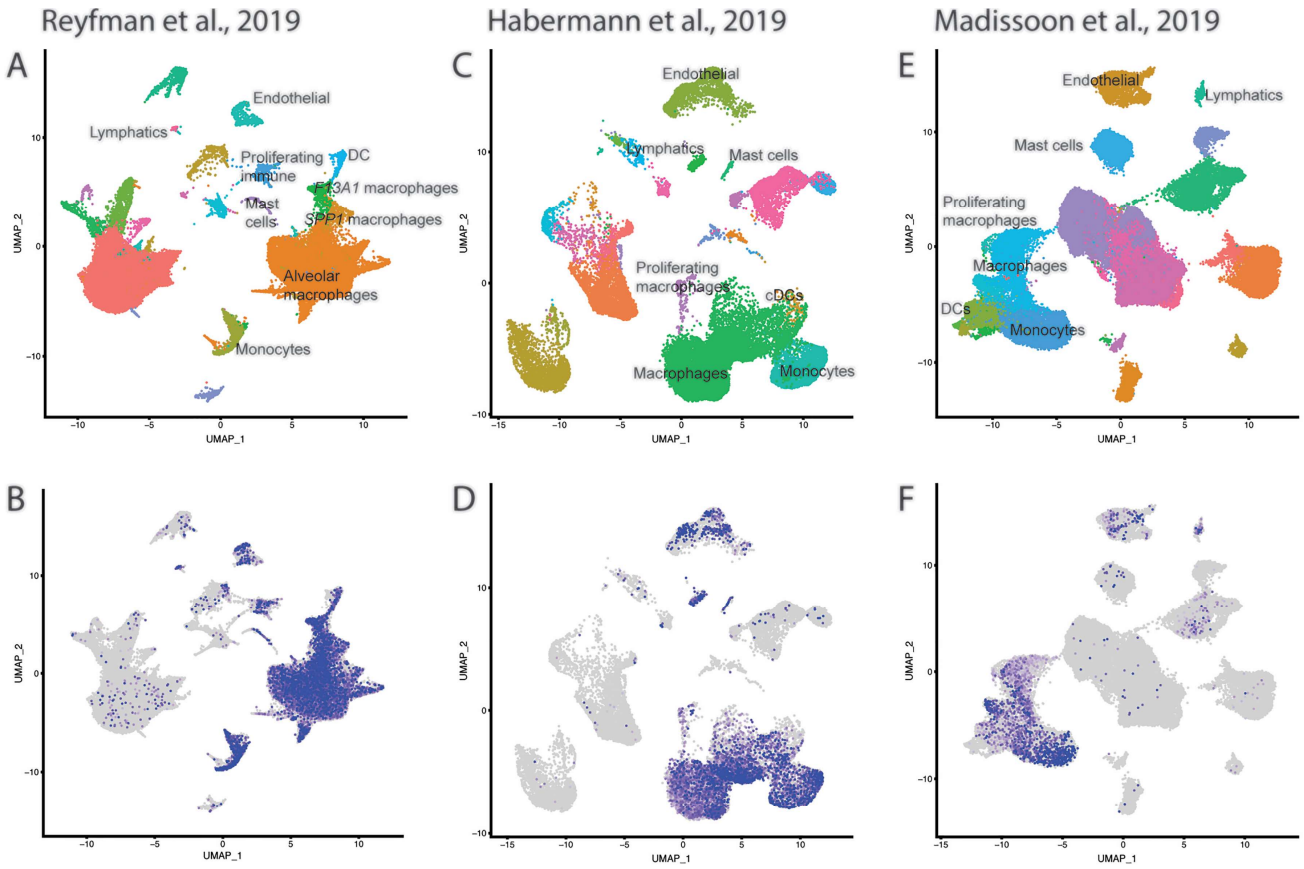

Suppl Figure 4

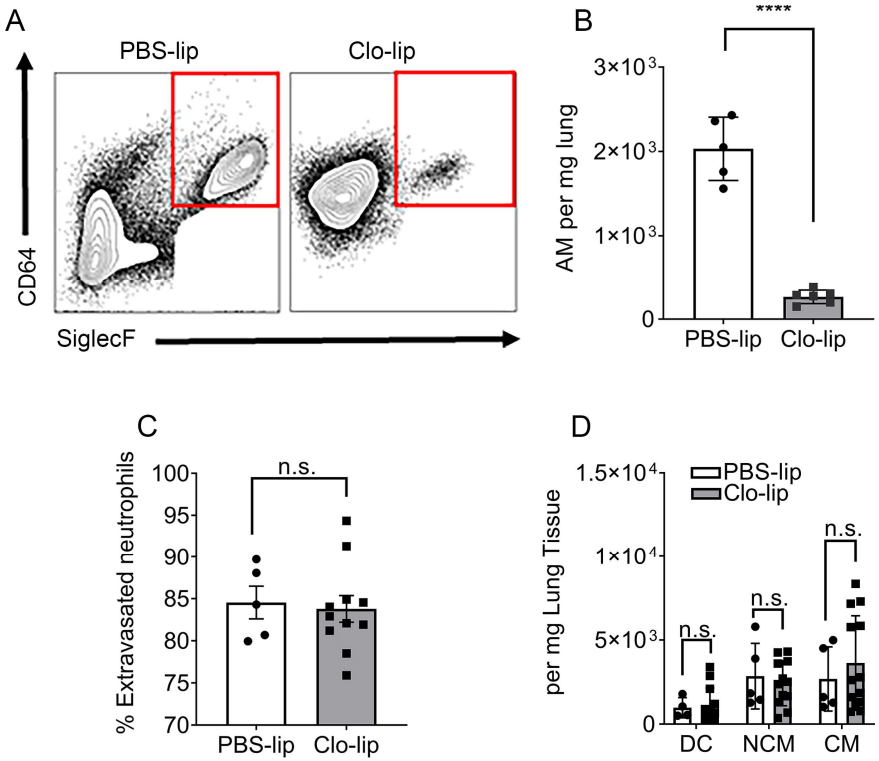

Suppl Figure 5

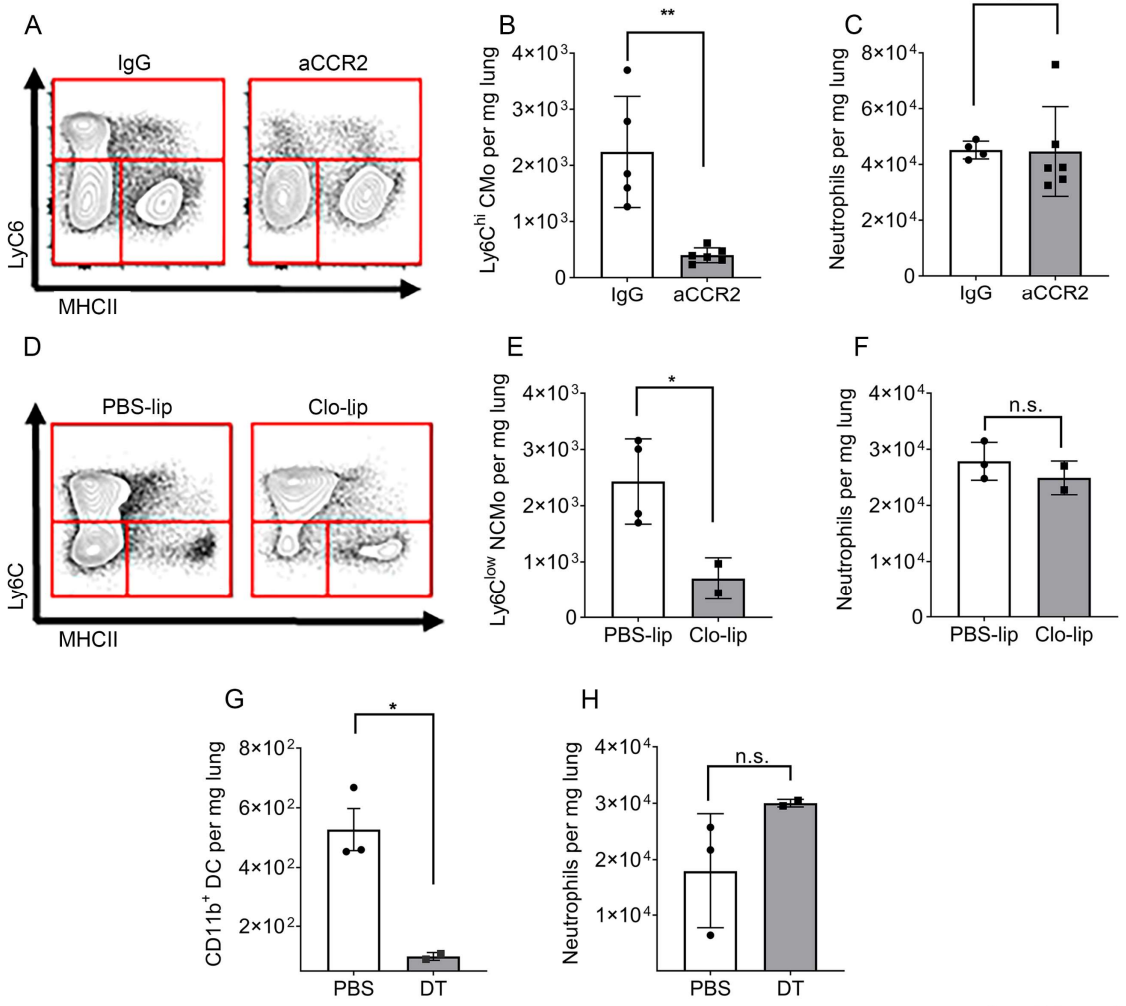

Suppl Figure 6

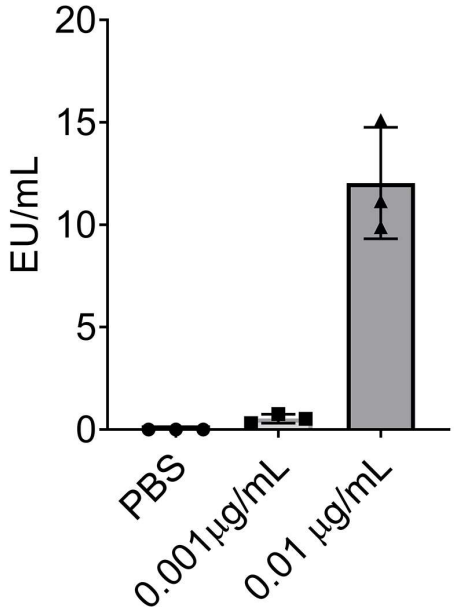

Suppl Figure 7

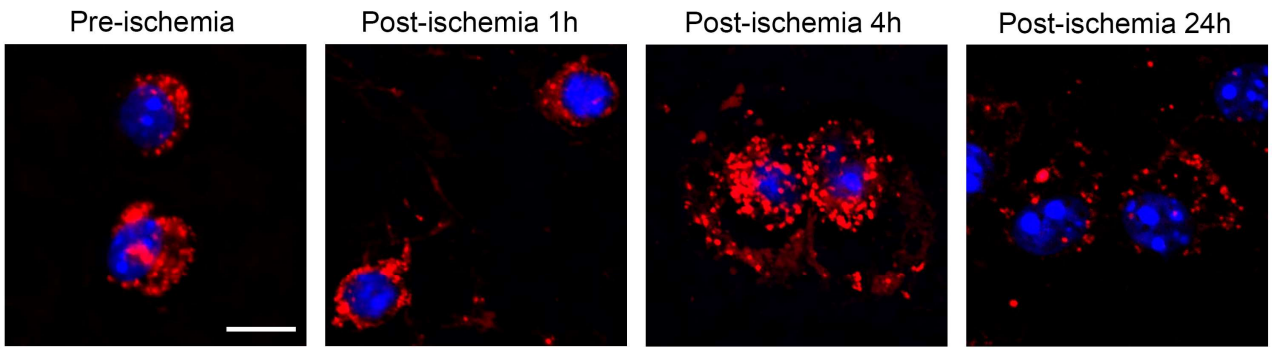

Suppl Figure 8

Pre-ischemia

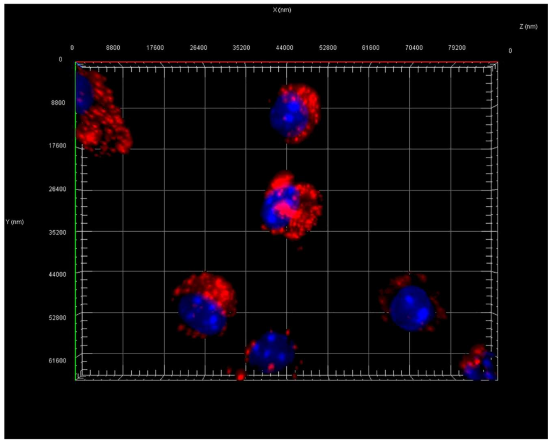

Post-ischemia 1h

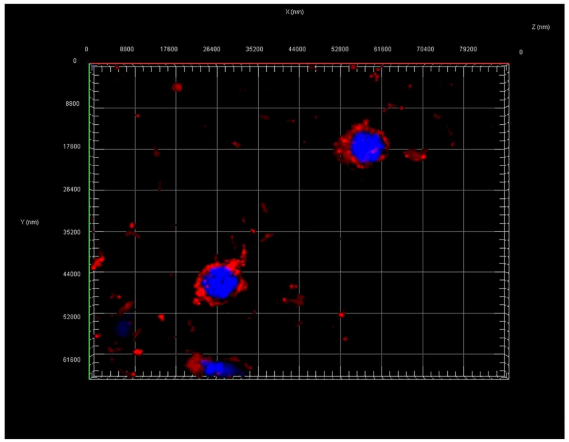

Post-ischemia 4h

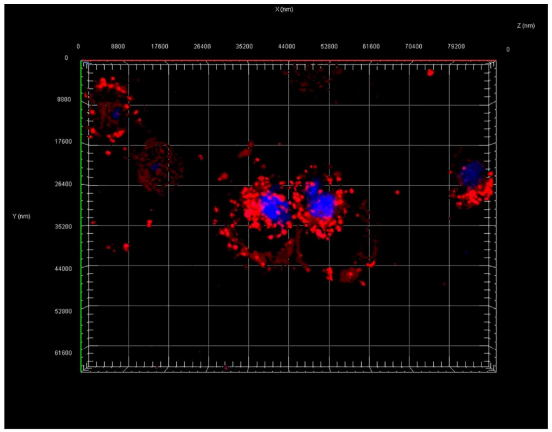

Post-ischemia 24h

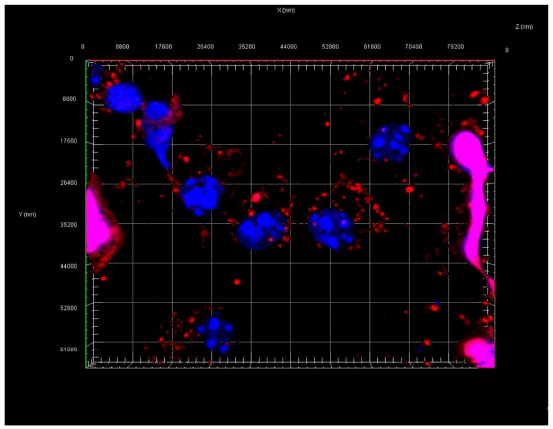

Suppl Figure 9

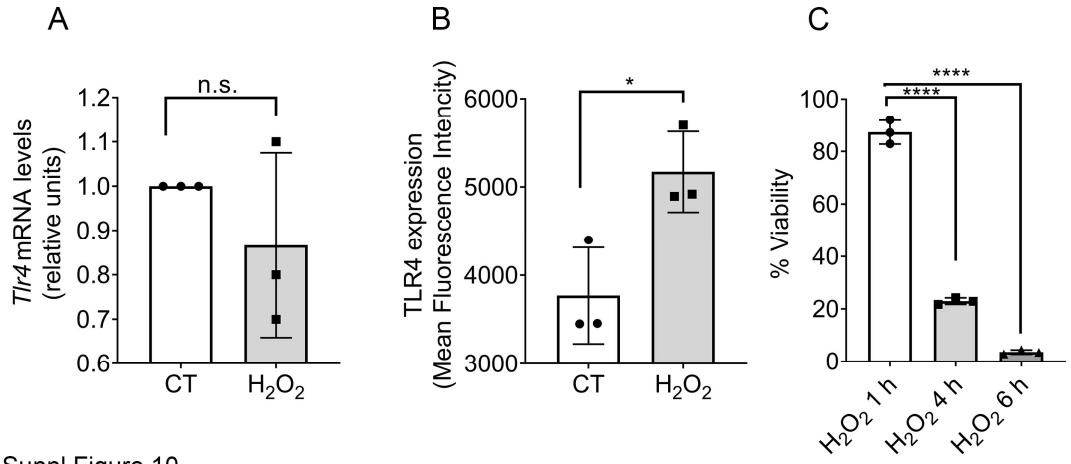

Suppl Figure 10